Chapter 1

Introduction

1.1 General background

Approximately 74% of global CO_2 emissions are caused by road vehicles (Fig. 1a). This has led to the implementation of stringent global regulations aimed at minimizing emissions from these vehicles [1]. The main weight factor in vehicles like cars is steel, which accounts for more than 46% of the body's weight [2] (Fig. 1b). So, the modern automotive market demands enhancement in fuel efficiency and reduction in greenhouse gas emissions through vehicle weight reduction. In this regard, down-gauging of the material could reduce the weight, but to maintain the minimum stiffness, this approach is not acceptable. The development of new steel grades, particularly low-density alloys, offers the potential to reduce the weight of automobile bodies, thereby increasing fuel efficiency and reducing carbon dioxide emissions. As a result, low-density steels have become a key focus in the automotive sector, owing to their lightweight nature and superior mechanical properties compared to those of conventional steels [3-4].

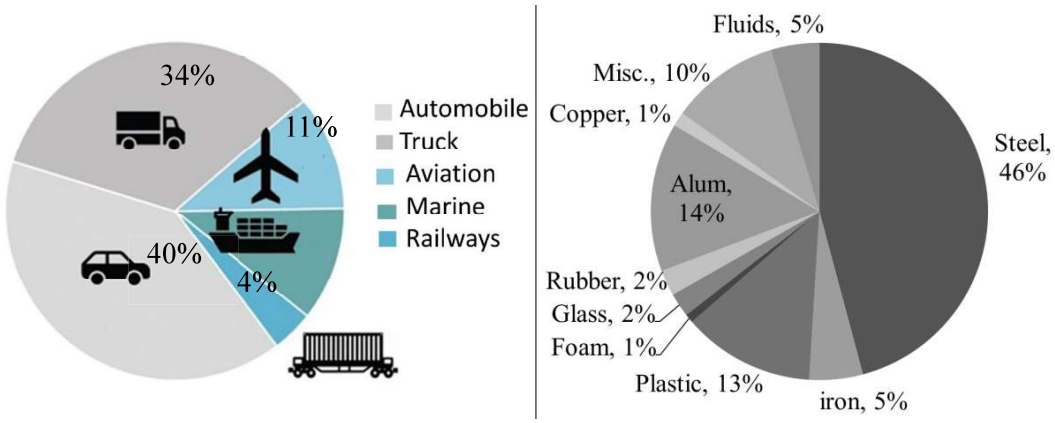

Fig. 1: (a) Global CO_2 emission [1], (b) material contents in car [2].

Steels used in the automobile industry can be classified based on their strength into three categories: (a) low-strength steels, such as mild steel and interstitial free (IF) steel, (b) conventional high-strength steels (HSS), such as bake hardening and high strength low alloy steel, and (c) advanced high-strength steels (AHSS), such as dual phase, complex phase, transformation-induced plasticity, twinning-induced plasticity, and martensitic steels [5-6].

Many developments have been made since the 1950s in the design of AHSS to replace conventional Fe-Cr-Ni steels. Replacing nickel with manganese and chromium with aluminium is most common due to less difference in alloying effect from a metallurgical point of view. These steels were also found to be very less expensive and were named low-density steel. Ham and Cairns first developed Fe-34Mn-10Al-0.76C steel in 1958 as a replacement for Cr-Ni steels [7]. This steel exhibits excellent corrosion and oxidation resistance. In 1969, Kayak et al. developed Fe-(25-30)Mn-(8-10)Al-1C steel for applications such as springs, gears, and landing gears, showcasing precipitation hardening and good oxidation resistance [8]. In 1985, Kim et al. introduced Fe-30Mn-5Al-0.3C-0.1Nb steel for cryogenic applications, known for its high strength and elongation at lower temperatures [9]. In 2000, Frommeyer and Brux developed Fe-(18-28)Mn-(9-12)Al-(0.7-1.2)C steel for automotive body frames, offering low weight and high crashworthiness [10]. Since the 2000s, research laboratories worldwide, both academic and industrial, have been dedicated to understanding and developing these steels. In 2013, Kim et al. provided a comprehensive review of Fe-Mn-Al-C steels for automotive applications [11]. Recent special issues in Scripta Materialia [12] and JOM [13] have focused on low-density steel. During the last two decades, much effort has been directed towards the development of ductile lightweight steels with high strength and reduced density for structural applications, automotive, military, and other transportation industries. Figure 2 illustrates the well-

known banana curve of various steels representing elongation with respect to tensile strength.

The main alloying elements which reduce the weight of steel by more than 20% and density to 6.5 g/cc are manganese (7.21g/cc), aluminium (2.7 g/cc), carbon (2.26 g/cc) and silicon (2.3 g/cc) [14]. The reduced density is due to light elements altering the lattice parameter of steels and decreasing density because of their low atomic masses. For instance, adding 12% aluminium to iron results in a 17% density reduction; 10% is due to lattice expansion, and 7% is attributed to the lower atomic mass.

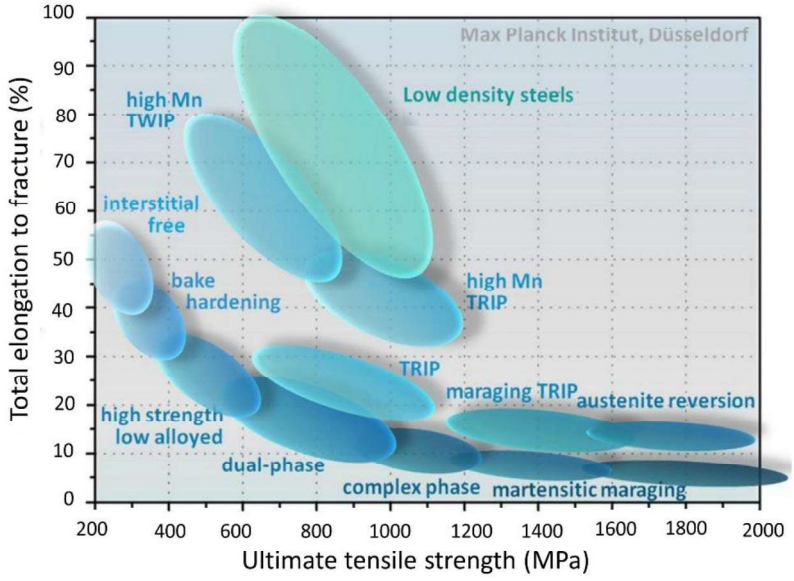

Fig. 2: Elongation vs. ultimate strength of different steels [12-13].

Fe–Al–Mn–C lightweight steel can be classified into four categories based on their matrix phase constituents: (i) ferritic steels, (ii) ferritic-based duplex steels, (iii) austenitic-based duplex steels, and (iv) austenitic-based steels [14]. Table 1 provides a summary of these categories along with their respective strength and total elongation (TE). The microstructures of ferritic steel are characterized by a high fraction of ferrite (δ) matrix, a

small amount of austenite (γ) matrix, and some finely dispersed k-carbide precipitates [14-16]. In contrast, the microstructures of austenitic steel are characterized by a high fraction of austenite matrix, a small amount of ferrite matrix, and some finely dispersed k-carbide precipitates.

Table 1: Different categories of low-density steels [14].

S.no	Category	Chemical composition range (wt. %) Al	Mn	C	Mech. Properties UTS (MPa)	TE
1	Ferritic steels	5-9	< 5	< 0.05	200-600	10-40%
2	Ferrite based duplex	3-7	2-12	0.05-0.5	400-900	10-40%
3	Austenite based duplex	5-10	5-30	0.4-0.7	800-1300	10-40%
4	Austenitic steels	5-12	12-30	0.6-2.0	800-1500	30-80%

However, the stability of both ferrite and austenite phases depends on the influence of all the alloying elements [17]. High aluminium content combined with medium manganese levels typically results in the formation of duplex (δ +γ) phases in the Fe-Mn-Al-C alloy system [18], [19].

Thermodynamic studies indicate that steel with Mn and Al content above 5 wt% forms a single-phase body centred cubic (BCC) ferrite during prolonged annealing at high temperatures [20- 21]. A single ferrite phase is undesirable because it can degrade toughness, corrosion resistance, and weldability properties. Medium-Mn and high-Mn steels possess excellent mechanical properties with a wide range of tuneable parameters, including yield strength (YS) (375–1850 Mpa), ultimate tensile strength (UTS) (765–1978 Mpa), and total elongation (1–80%) [21-22]. Austenitic steels exhibit a single austenitic phase at hot working temperatures and primarily consist of an austenitic phase with traces of δ-ferrite, k-carbide, and β-Mn phases[8], [23]. Slow cooling leads to k-carbides and

ferritic phases forming, which typically appear along the austenitic grain boundaries and within the austenite matrix, reducing ductility and toughness. Therefore, these steels are generally WQ from the solution temperature (900–1100°C) to prevent the precipitation of coarse k-carbide [14], [24].

Various aspects of Fe-Mn-Al-C low-density steel and viewpoints have been published to understand the deformation behaviour at the microstructural level to achieve desired mechanical properties to serve the automotive applications [4], [6-8]. In thermomechanical processes, nucleation and grain growth occur to replace the deformation in the material via static recrystallization. However, there is a limitation of minimum grain size which can be achieved (limited to 5-20 μm) [25-26]. To eradicate these difficulties, grain refinement via dynamic recrystallization is continuously adopted in the area of industrial research [27]. Dynamic recrystallization that takes place during deformation at elevated temperature ($>0.5T_m$) is known as discontinuous dynamic recrystallization (DDRX) and initiates the nucleation and grain growth phenomena which are generally observed in engineering metals such as steels, Ti-alloys, Mg-alloys and Ni-alloys [28-29].

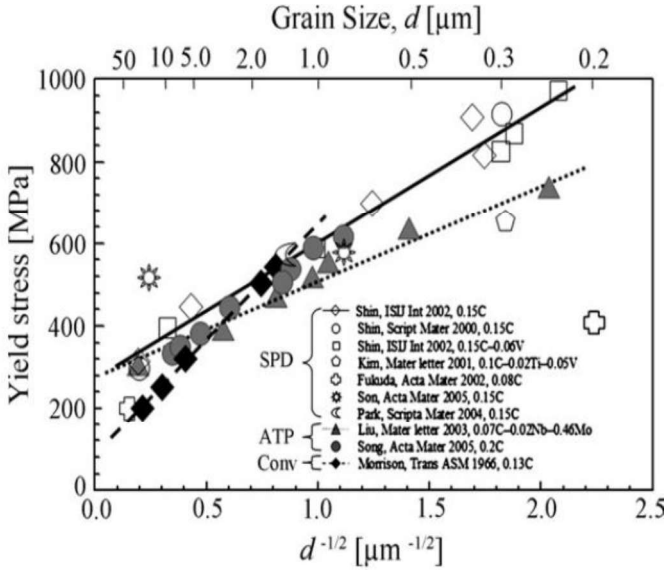

Fig. 3: Grain size dependence of ductility for steels [26].

From Fig. 3, it can be inferred that grain refinement must be reduced to less than 10 μm to achieve higher yield strength. This level of refinement can only be achieved through severe plastic deformation (SPD) processes [30-31]. Ultrafine-grained metals and alloys exhibit excellent mechanical properties, including high strength, fracture toughness, wear resistance, super-plasticity, and corrosion resistance. Recent studies on strengthening through microstructural development have introduced various SPD techniques. During SPD at temperatures below the melting point, grain refinement occurs via continuous dynamic recrystallization (cDRX), which becomes more pronounced as the deformation temperature decreases [32]. In cDRX, instead of traditional nucleation and grain growth, the original grains are continuously subdivided into smaller subgrains due to dislocation movements and rearrangements. This subdivision occurs progressively as deformation advances [33] .

There are SPD techniques such as equal channel angular pressing (ECAP), high pressure torsion (HPT), twist extrusion, accumulative roll bonding (ARB), and others. Most of them are limited in their ability to collect data about flow stress, material homogeneity, volume consistency. They are typically restricted to laboratory experiments [30], [34-38]. MAF has proven its advantage in producing bulk material for the automotive industry without changing the shape and size of the processed material. Although, it is a complicated 3-D forging process with unstable and non-uniform plastic deformation, it has been used to improve the mechanical properties after multiple MAF passes of various materials, including copper, magnesium, aluminium, iron, and titanium alloys [38-42].

The MAF is done in three mutually perpendicular directions, and compressing in each direction is referred to as one pass. Completing three passes one by one comprises one cycle. It is carried out by compressing the workpiece in a die to a fixed strain at the initial.

Then, the sample is removed from the die, rotated 90° vertically and horizontally, reinserted in the die, and pressed to the same strain. It's basically the recurrence of the free forging process numerous times with the alterations of axes of loading, including setting and pulling operations usually applied in the temperature range of 0.1 to 0.5 times the absolute melting temperatures of materials. In high-strength materials such as steel, MAF is likely to be performed at temperatures close to the recrystallization range (between 600°C and 700°C) [43-44]. This temperature range is selected for the forging process because it enhances ductility for carrying multiple forging passes and helps prevent the formation of undesirable martensite. However, more MAF passes are necessary for improved strength and refined grains. An alternative approach is to execute MAF under warm temperature conditions. However, the substance should be quite ductile. In this regard, austenitic Fe-Mn-Al-C low-density steel is particularly suitable for microstructural refinement processes due to its high ductility, exceeding 80% at room temperature [45]. The higher ductility of this material can possibly allow a greater number of forging passes, leading to grain refinement and improved mechanical properties within a single composition at various strain levels. Consequently, austenitic Fe-Mn-Al-C low-density steel can withstand more forging passes compared to conventional austenitic steel.

Going with MAF experimentation is a lengthy and costly process. Achieving higher strain in a material requires multiple passes, with experimental procedures repeated multiple times. Additionally, optimizing the operating or deformation parameters at each step is crucial. These parameters, which include variables such as temperature, strain, strain rate, and others, significantly influence the equivalent strain during material deformation. Even slight variations in these parameters can lead to different mechanical behaviour responses. Manually optimizing the process parameters to achieve better results becomes a complex challenge. Also, the die walls in the MAF process limit plastic flow, causing discrete plastic

strain in different regions of material. Bulk deformation introduces triaxial stress during compression, and upon unloading, generates internal residual stress that remains inside the material as internal stress distribution [46]. All these elements work together to cause complex changes in the interior structure of materials during a shaping operation [47]. So, understanding the equivalent plastic strain during this process has become a prime importance for gaining insights into how to adjust the parameters of deformation to provide efficient and better-quality results. Finite element analyses (FEA) and experiments have shown that the deformation of SPD-processed materials is nonhomogeneous. Some portions of the samples are more strained compared to others [48]. Analytical methods, which rely on certain assumptions, often fail to accurately reveal the stress behaviour of materials. Experimental methods, while more precise, can be costly in terms of equipment, materials, tools, and time. Finite element (FE) simulation offers an effective and realistic alternative for analysis. Using the FEM, it is possible to understand deformation behaviour and optimize key process parameters while saving both time and costs.

Furthermore, when selecting the optimal design scenario, researchers often incorporate constitutive models in FEM that include information on the underlying mechanisms governing the material's deformation process. Some of well utilised model in SPD techniques are as follows:

1. Zerilli-Armstrong model
2. Bodner-Partom model
3. Khan-Huang (KH) model
4. Johnson-Cook (J-C) model

The flow stress models mentioned above perform well under deformation conditions involving mechanisms such as strain hardening, strain rate effects, and thermal softening. However, MAF deformation is a complex phenomenon that also involves mechanisms like

grain refinement, dislocation density, and phase transformations, operating at both micro and macro scales. To achieve more accurate simulation results, it is essential to incorporate these additional underlying mechanisms into the flow stress model.

Finally, in the present work, a comprehensive assessment of the microstructure-mechanical properties, along with FE simulation, is necessary to evaluate the suitability of Fe-Mn-Al-C low-density steel for automotive applications.

1.2 Thesis organization

The thesis comprises nine chapters, with the Introduction as **Chapter 1**.

Chapter 2 discusses the literature review, which has been split into four sections. The first section emphasises the significance of the alloying element of Fe-Mn-Al-C low-density steel, particularly in the domain of material selection. It covers details of the literature dealing with a mass fraction of manganese, aluminium, and carbon required in a base iron for manufacturing austenitic low-density steel. Further, it covers a detailed discussion about the formation of phases like ferrite and carbides, which regulate the mechanical properties of Fe-Mn-Al-C steels. The second section includes different strengthening mechanisms like grain boundary strengthening, dislocation strengthening, solid solution strengthening, and precipitate strengthening that give rise to the tensile strength of Fe-Mn-Al-C steels during static or dynamic recrystallization. The third section deals with the grain refinement and deformation behaviour of steels during MAF and the effect of strain rate and temperature. It also covers the effect of residual stress in a material developing during the MAF process. The fourth section deals with the constitutive relation for flow stress prediction during MAF.

Chapter 3 details the melting, casting and heat treatment procedures for the selected compositions. Then, the workpiece for MAF, die design, sample for tensile test and microstructural characterization are stated. Further, MAF procedures and the techniques

of triaxial residual stress analysis by XRD are discussed in a structured way. In addition, a method to evaluate the optimised constants of the J-C material model and the formulation of the required modified J-C model for an MAF process is discussed. Finally, the FE modelling approach of MAF procedures for the evaluation of flow stress and residual stress is presented.

Chapter 4 focuses on the microstructure and mechanical behaviour of Fe-30Mn-9Al-0.8C and Fe-20Mn-10Al-1C low-density steels. This chapter discusses the microstructural parameters for biaxial forging and solution-treated samples for the two steels. Then, the mechanical properties are evaluated.

Chapter 5 discusses the evaluation of J-C parameters for the plastic deformation of Fe-30Mn-9Al-0.8C low-density steel. Experimental data is utilized to determine the characteristic parameters necessary for establishing the empirical J-C model. The reliability of these J-C parameters is further enhanced using a GA based optimization technique. Subsequently, the improved J-C constitutive equation is employed in numerical simulations (using ABAQUS Explicit software) for two different tensile tests.

Chapter 6 shows the deformation of the Fe-Mn-Al-C low-density steel using MAF. Then, the microstructural examination is conducted using an optical microscope, XRD and EBSD. The evolution of mechanical properties is investigated based on the number of MAF passes. Strengthening mechanisms, such as grain refinement and dislocation density, are evaluated from the observed microstructural phenomena.

Chapter 7 conducts the FE simulation of MAF for Fe-30Mn-9Al-0.8C low-density steel using a microstructure-based modified J-C constitutive equation. A modified J-C model incorporating the effects of dislocation density and grain size has been formulated to predict the flow stress and material strength achieved after each MAF pass. Subsequently, FEA is performed to replicate the actual microstructural evolution during the MAF process.

Chapter 8 investigates the residual stresses in multiaxially forged Fe-30Mn-9Al-0.8C low-density workpiece through the XRD and the FEM. The interplanar spacing (d) and $\sin^2\psi$ values obtained from XRD are employed in triaxial stress analysis to determine all stress components. For FEM simulation, a microstructure based modified Johnson-Cook model is employed to predict the residual stresses.

Chapter 9 contains the conclusions and the scope for future work.